RSC Sustainability

ROYAL SOCIETY OF CHEMISTRY

PAPER

View Article Online
View Journal | View Issue

Cite this: *RSC Sustainability*, 2023, **1**, 1982

Fast and simple preparation of microparticles of $KHCO_3$ by a freeze-dissolving method with single solvent or additional antisolvent†

Jiaqi Luo, [a] Qifan Su,[a] Qiushuo Yu,*[a] Xinyue Zhai,[a] Yuan Zou[a] and Huaiyu Yang *[b]

Received 8th July 2023
Accepted 6th September 2023

DOI: 10.1039/d3su00234a

rsc.li/rscsus

Microparticles featuring specific attributes are essential for the chemical industries. Microparticles of $KHCO_3$ were prepared by a freeze-dissolving method, with one solvent or with additional antisolvent. Firstly, $KHCO_3$ aqueous solution was dripped into liquid nitrogen to prepare ice spherical particles, and additional antisolvent, ethanol, was used to dissolve the ice scaffolding to isolate the microparticles of $KHCO_3$. In this work we have developed a new freeze-dissolving method with only one solvent, water. After formation of ice particles, a low-temperature saturated aqueous solution of $KHCO_3$ was used to dissolve the ice in frozen spherical particles at low temperature to isolate the microparticles. Both freeze-dissolving methods were 100 times faster and more energy-efficient than the traditional freeze-drying method. The microparticles of $KHCO_3$ obtained by the freeze-drying method and freeze-dissolving with antisolvent and with saturated solution were characterised with SEM and the particle size distributions were compared.

Sustainability spotlight

This work demonstrates a fast, efficient and energy-saving technology for the production of microparticles. The freeze-dissolving methods can produce $KHCO_3$ microparticles of similar size distribution for only 1% of the time period and 1% of energy consumption compared with the traditional freeze-drying method. The freeze-dissolving in saturated solution method, with only one solvent, allows fast application for not only salts but other chemicals, organics and pharmaceuticals. The new technology can ensure sustainable consumption and production patterns, which align with UN SDG 12.

Introduction

Particle production technology accounts for a significant value for the chemical industry.[1–5] Microparticles have been reported to have advantages over normal powder[6] in terms of storage and transportation. Microparticles have a series of special properties because of their ultra-high specific surface area,[7–9] leading to fast chemical reaction speed, strong surface adsorption capacity and large solubility. Microparticles can be produced by mechanical crushing of normal powder[10–12] or be directly manufactured by physical and chemical methods.[13–15] As the traditional process for preparing microparticles still has challenges on cost, efficiency and product properties such as size distribution, innovative methods are required[16–19] to manufacture microparticles. One widely used method is freeze-drying (FDry).[20,21] Firstly, an aqueous solution with certain concentration of target product is frozen into ice particles, with a structure of ice scaffolding mixed with microparticles formed during the freezing. Then, the ice scaffolding is sublimated under vacuum condition at low temperature, and the microparticles remain.

In previous work, we demonstrated the freeze-dissolving method.[22] With the same first step to form ice particles, the second step is to dissolve the ice particles in an antisolvent at temperature below 283.15 K, and then the microparticles are easily isolated after filtration. Compared with the traditional FDry method, the freeze-dissolving in antisolvent (FDas) method is much faster, with much smaller facility footprint and much less energy consumption. Moreover, the products of the FDas method were similar to or even better than the products of the FDry method as demonstrated in previous works.[22,23] However, for the FDas method, it is essential to find an antisolvent, in which the target compound has much lower solubility (ideally close to zero), because for an antisolvent with moderately low solubility it could still be possible to dissolve some of the microparticles, especially tiny particles, during the second step. For inorganic salt systems, it is not difficult to find an antisolvent such as organic solvents, like ethanol or acetone. However, for organic compounds or organic salts, it can be

[a]School of Chemical Engineering, Northwest University, Taibaibei Road 229, Xi'an, 710069, Shaanxi, China. E-mail: yuqiushuo@nwu.edu.cn

[b]Department of Chemical Engineering, Loughborough University, Loughborough LE11 3TU, UK. E-mail: H.yang3@lboro.ac.uk

† Electronic supplementary information (ESI) available. See DOI: https://doi.org/10.1039/d3su00234a.

challenging to find a perfect antisolvent, and binary solvents can induce liquid–liquid phase separation, hindering nucleation and crystallization.[24,25] In summary, it is challenging to identify a suitable second solvent as antisolvent for some systems, especially for complex molecules, such as organics and proteins,[26,27] and it requires more experiments and time to determine the solubility in the solvent mixture to design and control the freeze-dissolving process with the FDas method.

In this paper, we propose a new freeze-dissolving method using a saturated solution to dissolve the ice particles, which can be easily applied to more systems. The freeze-dissolving in saturated solution (FDss) method was demonstrated by producing $KHCO_3$ microparticles with advantages of using only one solvent to save effort and time to identify a suitable second solvent as antisolvent and to design the freeze-dissolving process without extra solubility data of solvent mixtures. Similar to FDry and FDas, ice particles of $KHCO_3$ were produced in the first step of FDss. In the second step, the ice particles of $KHCO_3$ were dissolved in a low-temperature saturated solution of $KHCO_3$, and then the microparticles of $KHCO_3$ were easily isolated after filtration. Four concentrations, 0.3–0.5 g $KHCO_3$ per g water, and different sizes of ice particles, 0.01 and 0.04 cm^3, were used to compare three methods, FDry, FDas and FDss. The size distribution and PXRD patterns of all the microparticle products were determined and the particles were observed by SEM. The mechanisms of particle formation are discussed, and sustainabilities of these methods were analyzed.

Materials and methods

Materials

Ethanol was purchased from Tianjin Damao Chemical Reagent Factory (purity >99.7%). Potassium bicarbonate, $KHCO_3$, was purchased from Tianjin Baishi Chemical Co. Ltd (purity >99.5%). Liquid nitrogen (purity >99.9%) was purchased from Xi'an Aier Industrial Gas Co. Ltd. All chemicals were used without further purification. Distilled deionized water (conductivity <0.5 μS cm^{-1}) was used.

Method

Potassium bicarbonate aqueous solutions were prepared at 328.15 K, with different weights of 3, 4, 4.5, and 5 g of $KHCO_3$ in 10 g water. Then each solution was transferred by a pipette into an insulated pan with 10 mL of liquid nitrogen to form ice spherical particles. Two droplets with average masses of 0.0135 g and 0.0425 g were selected and dropped into the liquid nitrogen. All droplets quickly sank into the liquid nitrogen to form frozen spherical particles with mainly two different volumes. The average mass was calculated based on 300 frozen spherical particles of each size, the uncertainty was less than 10%, and the corresponding average volumes were 0.01 and 0.04 cm^3, respectively.

Three techniques, FDry (freeze-drying), FDas (freeze-dissolving in antisolvent) and FDss (freeze-dissolving in saturated solution), were used to obtain microparticles from the ice spherical particles, shown in Fig. 1. With FDry method, frozen spherical particles were put into a freeze dryer (FD-1A-50, Beijing Boyikang Experimental Instrument Co. Ltd, China) for 24 h for sublimation of ice, with microparticles remaining. With FDas method, the frozen ice particles were poured into ethanol (mass 7 times more than that of the ice frozen particles, $\mathbf{R}_{ice/as}$=1:7,) at 253.15 K, and stirred continuously. With FDss method, the frozen particles were dissolved in saturated $KHCO_3$ solution at 275.15 K, and stirred continuously. For both FDas and FDss methods, the ice scaffolding in the frozen ice particles were dissolved for less than 10 min, and the $KHCO_3$ particles were filtered with PTFE (Whatman) with a 1 μm pore size during 5 min.

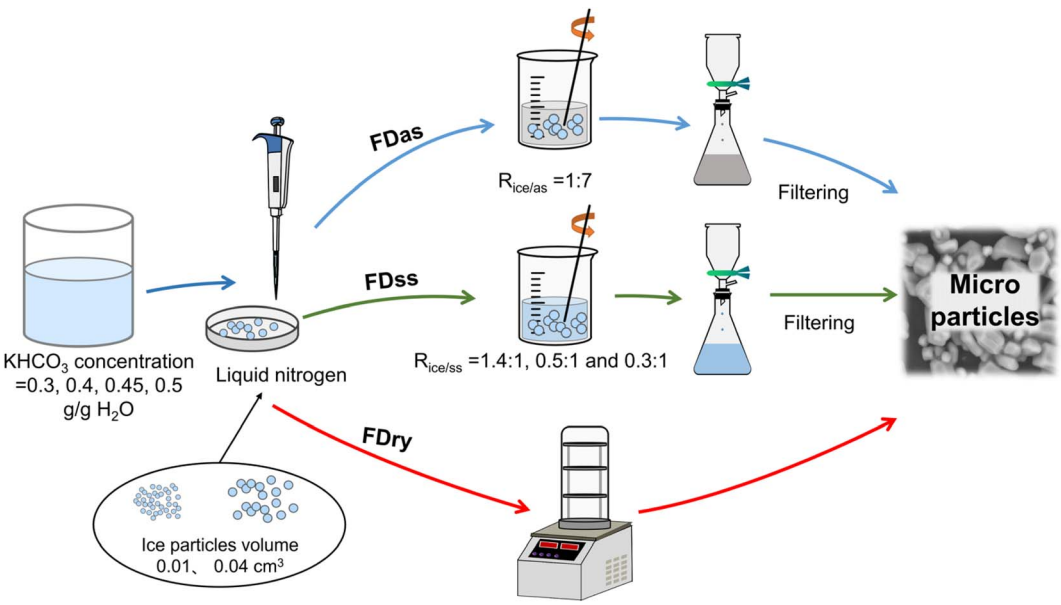

Fig. 1 Schematic diagram of experimental setup for three methods of freeze-drying, FDry, freeze-dissolving in antisolvent, FDas, and freeze-dissolving in saturated solution, FDss.

For the antisolvent crystallization method,[24,26] $KHCO_3$ solution of 0.5 g g^{-1} was poured into pure ethanol at room temperature under stirring of 400 rpm. The solid particles were obtained after filtration.

The $KHCO_3$ ice particles produced from the aqueous solutions (4 g in 10 g water) were dissolved in different amounts of saturated solution to investigate its influence. The mass of $KHCO_3$ saturated solution used for dissolving frozen particles was 10 g, 30 g and 50 g with different ratios, $\mathbf{R}_{ice/ss}$, of the mass of ice spherical particles to the mass of $KHCO_3$ saturated solution: 1.4 : 1, 0.5 : 1 and 0.3 : 1, respectively.

Characterization

The morphologies of the particle products were characterized with a scanning electron microscope (TM3000, Hitachi High Technologies Co. Ltd, Japan). The particles were analyzed using the powder X-ray diffraction at room temperature, with 40 kV and 40 mA. The scan rate was 8° min^{-1}. About 0.5 g of particles was added to an ethanol solution, which was then dispersed in an ultrasonic disperser for 5–10 min, and no influence was observed with a longer dispersion period (ESI, Table S1†). Each sample was measured three times using a laser particle size analyzer (Master Sizer 2000).

Density test

The particles prepared by FDss, FDas and FDry were filled into a measuring cup until it was full. The mouth of the cup was scraped with a straightedge. The bulk density of particles was calculated using the following equation:

$$\rho_b = \frac{m_1 - m_0}{V} \quad (1)$$

where ρ_b is the bulk density, m_1 is total mass of the measuring cup and particles, m_0 is mass of the measuring cup, and V is volume of the measuring cup.

Then, the measuring cup with particles was filled with ethanol slowly until it was full. The granule density of particles was calculated by:

$$\rho_g = \frac{m_1 - m_0}{V - \frac{m_2 - m_1}{\rho_e}} \quad (2)$$

where ρ_g is granule density, m_2 is total mass of the measuring cup, water and particles, and ρ_e is density of the ethanol.

Angle of repose measurement

The angle of repose was calculated using the fixed diameter method with the following equation:

$$\theta_r = \text{arc } tan\left(\frac{h}{r}\right) \quad (3)$$

where θ_r is angle of repose, h is height of accumulated particles formed by particles falling on a circular flat plate with fixed size through a funnel, and r is the radius of the circular flat plate.

Results and discussion

Fig. 2 shows that with low-concentration solutions of 0.3 and 0.4 g $KHCO_3$ per g water, the size distributions of particles obtained by FDss were narrowest, and the size distributions of those obtained by FDry method were narrower than those obtained by FDas method. The product average sizes obtained from these three methods were similar and products obtained by FDss were slightly bigger than those obtained by the other two methods, and the products from FDas had overall the smallest average size.

For the products of the same method, with an increase of the concentration, the size of microparticles tended to increase, as shown in the size distributions and SEM images in Fig. 2. For products from solutions with equal concentrations, fewer agglomerations were observed in the microparticles obtained by the FDss and FDas. With high-concentration solutions of 0.45 and 0.5 g $KHCO_3$ per g water, the size distributions of particles obtained by FDry were narrowest, and size distributions of those obtained by FDss and FDas were similar (Fig. 2(j–l)). There was no obvious change in the crystal morphology. With a solution of 0.5 g $KHCO_3$ per g water, the average sizes of products of the three methods were very similar.

Fig. 3 shows that with equal sizes of frozen spherical particles, the $KHCO_3$ microparticles obtained by the FDas and FDss methods were overall smaller than those obtained by the Fdry method. With a decrease in the sizes of the frozen spherical particles, the sizes of microparticles all decreased with the same method. As shown in Table 1, when the average size of frozen spherical particles was 0.01 cm^3, the average sizes of microparticles obtained by the three methods were 24.9 μm, 20.7 μm and 26.2 μm. These values were about half of those obtained with the average particle size of 0.04 cm^3 at the same concentration. The outcomes were consistent with $NaHCO_3$ system,[22] in which smaller ice particles resulted in smaller particles of $NaHCO_3$, as the microparticle formation was completed during the ice frozen steps, and for smaller droplets freezing rate was faster to form smaller ice particles.

Fig. 4(d) shows that two particle size peaks appeared when the value of $\mathbf{R}_{ice/ss}$ was equal to 1.4 : 1, which was in agreement with Fig. 4(a) where both large crystals and small crystals were observed. With very high $\mathbf{R}_{ice/ss}$, the water from melting of the ice particles would dissolve some of the microparticles. Despite the dissolution of microparticles, the temperature of saturated solution decreased, which generated supersaturation to produce some crystals by cooling crystallization, and the crystal particles from cooling crystallization were always much bigger. The first peak at about 40 μm shows the diameter of the microparticles inside the ice particles and the second park at about 158 μm shows the crystals formed due to cooling crystallization of the saturated solution. When $\mathbf{R}_{ice/ss}$ was decreased to 0.5 : 1 or 0.3 : 1, the size of the microparticles by FDas and FDss was in a similar range to those obtained by FDry. At $\mathbf{R}_{ice/ss}$ of 0.5 : 1, the average particle size of microparticles was 42.9 μm, which was slightly smaller than those obtained at $\mathbf{R}_{ice/ss}$ of 0.3 : 1 (average particle size was 52.6 μm), due to dissolution of more

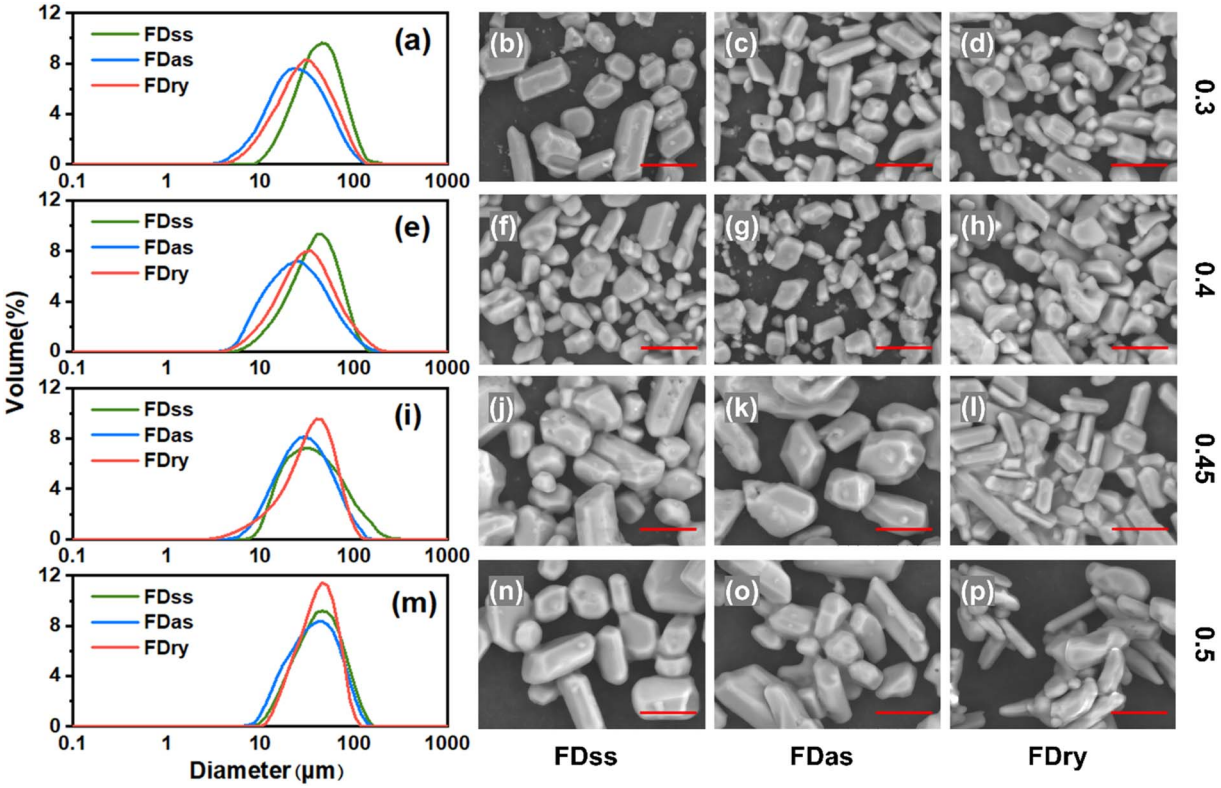

Fig. 2 Particle size distributions of $KHCO_3$ microparticles (frozen spherical particles with average size of 0.04 cm^3) from different concentrations of (a) 0.3, (e) 0.4, (i) 0.45, (m) 0.5 g $KHCO_3$ per g water and their corresponding SEM images: FDss (b, f, j and n); FDas (c, g, k and o); FDry (d, h, l and p) methods. Scale bar: 10 μm.

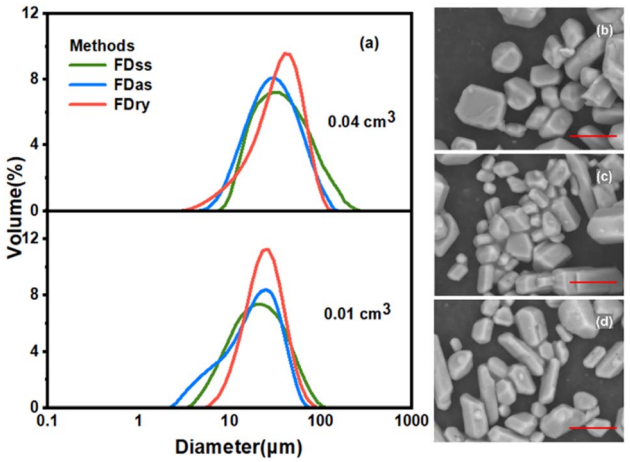

Fig. 3 (a) Particle size distributions of $KHCO_3$ microparticles isolated from frozen spherical particles with different average sizes of 0.04 (top) and 0.01 cm^3 (bottom) by the FDry, FDas and FDss methods and SEM images of particles from the FDss (b), FDas (c) and FDry (d) methods with average sizes of 0.01 cm^3 and 0.04 cm^3 of the frozen spherical particles. The concentration was 0.45 g g^{-1} for preparing the frozen spherical particles. Scale bar: 10 μm.

microparticles, especially in the small size range. As less ice was melted and the influence of the temperature change was limited, *i.e.* solubility remained the same, the melting ice increased the mass of the solvent, leading to dissolution of some of the microparticles. It is noted that based on the solubility of different systems, the optimised $\mathbf{R}_{ice/ss}$ can be different. In sum, due to the influence of temperature change and quantity of water due to melting of ice, the optimised condition to produce microparticles of $KHCO_3$ was at $\mathbf{R}_{ice/ss}$ of 0.5 : 1.

The microparticles were obtained with equal concentration condition, 0.5 g g^{-1}, from the three methods, FDss, FDas, FDry, as well as the antisolvent crystallization method. The average

Table 1 The average particle size of microparticles prepared by freeze-dissolving, free-drying and antisolvent crystallization methods

Freezing condition		Average particle size			
Concentration (g g^{-1})	V (cm^3)[a]	FDss (μm)[b]	FDas (μm)[c]	FDry (μm)	AS (μm)[d]
0.3	0.04	47.7	30.2	35.4	
0.4	0.04	42.9	31.4	39.1	
0.45	0.04	46.6	35.4	38.3	
	0.01	24.9	20.7	26.2	
0.5	0.04	48.4	43.1	44.2	
0.5	—				154.1

[a] The average sizes of the frozen spherical particles. [b] Mass ratio between ice and saturated solution, $\mathbf{R}_{ice/ss}$ = 1 : 2. [c] Mass ratio between ice and antisolvent solvent, $\mathbf{R}_{ice/as}$ = 1 : 7. [d] Antisolvent crystallization.

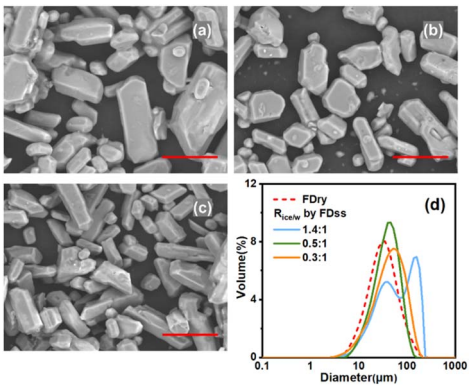

Fig. 4 SEM images of $KHCO_3$ microparticles isolated from frozen spherical particles with average sizes of 0.04 cm^3 by the FDss method for different $R_{ice/ss}$ of 1.4 : 1 (a), 0.5 : 1 (b) and 0.3 : 1 (c) and particle size distributions (d) for the FDry and FDss methods at different $R_{ice/ss}$. The concentration was 0.4 g g^{-1} for preparing the frozen spherical particles. Scale bar: 10 μm.

particle size of microparticles obtained by FDss and FDas was 48.4 μm and 43.1 μm, respectively, and the microparticle size distributions were narrow, shown in Fig. 5. $KHCO_3$ microparticles are widely used as dry powder fire extinguishing agent, and the sizes for applications are mainly in the range of 10–75 μm.[28–30] The average particle sizes obtained by FDss and FDas were in the range of 30–50 μm. The bulk densities, by eqn (1), of products obtained by FDss, FDas and FDry were in a similar range, 0.93 g mL^{-1}, 0.71 g mL^{-1} and 0.82 g mL^{-1}, respectively. The granule densities, by eqn (2), were also similar, 2.16 g mL^{-1}, 2.04 g mL^{-1} and 2.09 g mL^{-1}, respectively. The products were all of good fluidity, with angles of repose, by eqn (3), of 26.5°, 31.3° and 28.7°, respectively.

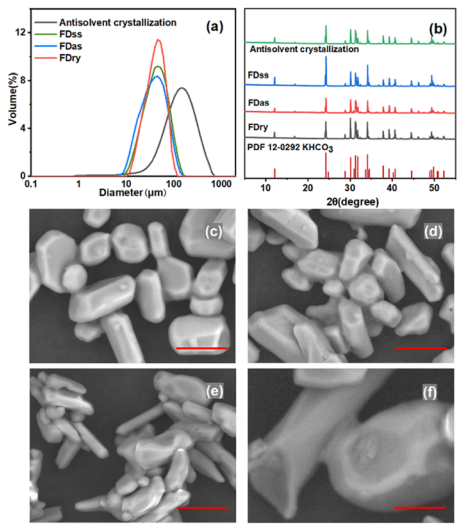

Fig. 5 Particle size distribution (a) of $KHCO_3$ microparticles obtained with different methods. PXRD patterns (b) and SEM images of particles from FDss (c), FDas (d), FDry (e) and antisolvent crystallization (f) with average sizes of 0.04 cm^3 of the frozen spherical particles, prepared with a solution at 0.5 g g^{-1}. Scale bar: 50 μm.

The particles with average size of 150 μm obtained by antisolvent crystallization were more than 4 times larger than the particles obtained by FDss, FDas and FDry methods. The big size of particles from cooling crystallization also supported the hypothesis that the second peak in the size distribution in Fig. 4 was due to the cooling crystallization. When $KHCO_3$ solution was added to ethanol at a higher rate, the supersaturation of the whole system became high, and then the accumulation of supersaturation could only be consumed rapidly by crystal growth. However, the supersaturation decreased with more $KHCO_3$ solution added into ethanol. With FDas, FDss and FDry methods, the superstation in ice particles was very high, and the nucleation and crystal growth completed in seconds or less, with nearly no growth time for the crystals inside. The PXRD patterns in Fig. 5(b) showed that the particles produced from all four methods were all crystalline with the same polymorph.

After the frozen ice particles were produced with microparticles inside, FDss, FDas and FDry can all be used to separate the microparticles out of the ice scaffolding. With FDry, the method was to sublimate the ice into vapor phase, requiring about 1440 min. With FDas, it was to dissolve the ice scaffolding with the antisolvent, which was ethanol, at a temperature about 20 K lower than the ice point. With FDss, it was to dissolve the ice scaffolding with the saturated solution at low temperature, about 10 K above the ice point. The dissolving processes were both fast, and the whole process including filtration only needed about 15 min, which was only about 1% of the time period compared to the application of FDry. The energy consumption for production of 1 g microparticles was estimated to be 4.3×10^4 kJ for FDry, 3.0×10^2 kJ for FDas and 2.4×10^2 kJ for FDss, based on the lab operations (details in Table S2†). The energy consumption was much lower without the requirement of a vacuum, which was about 1% energy consumption for both FDas and FDss compared to the application of FDry.[22] Due to the dissolution process occurring at higher temperature, the energy consumption of FDss was even less than that of FDas. Comparing the FDss, FDas and FDry methods, the freeze-dissolving methods (FDss and FDas) did not require a vacuum, providing a rapid method for preparing microparticles with low energy requirements, leading to the benefit of sustainability, shown in Fig. 6.

For FDas, only one solvent (water) was used to obtain $KHCO_3$ (or $NaHCO_3$ (ref. 22)) aqueous solution. For the second solvent, it is easy to choose an organic solvent as antisolvent, as most salts do not dissolve in organic solvents. For applying this technology in producing target organic chemicals, drug micronization and food additives, if an organic solvent is chosen as the solvent (frozen particles are possible to form in liquid N_2), antisolvent can be difficult to choose, with low solubility and low melting point (below that of the organic solvent used to form frozen particles). However, if a saturated solution with the current organic solvent can be directly used, it will be much easier to operate without efforts on screening another suitable solvent. Therefore, the FDss method has the advantages of simple equipment requirements, easy operation,

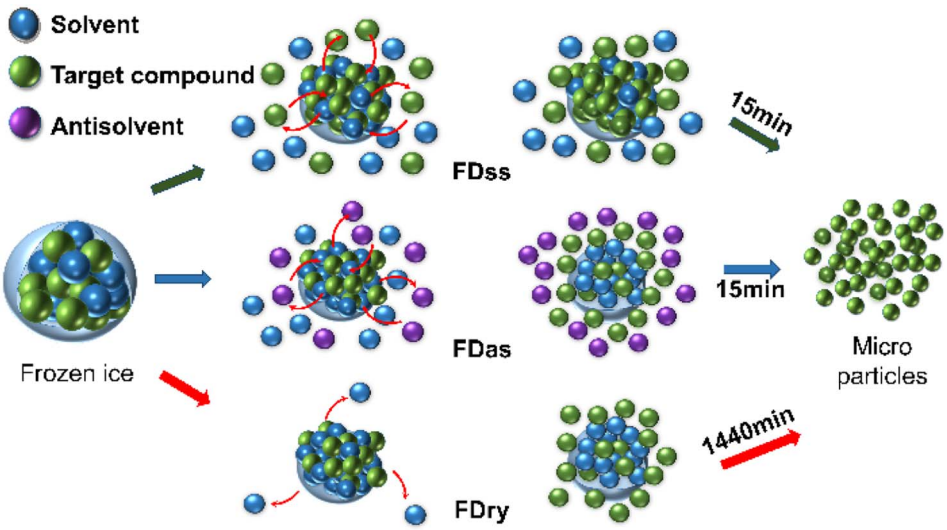

Fig. 6 Schematic diagram of the FDss, FDas and FDry mechanisms for the formation and isolation of microparticles.

low investment and low energy consumption, and a smaller amount of the saturated solution could be designed to recover the particles with high yield. Further research is needed for optimizing the saturated solution temperatures, freezing process, and ice particle sizes to produce smaller microparticles.

Conclusions

A new freeze-dissolving in saturated solution method was demonstrated in this work, using only one solvent to isolate microparticles of $KHCO_3$. This method is simple and fast with energy- and cost-efficiency advantages. In the first step, frozen spherical particles, from $KHCO_3$ aqueous solution, were obtained. Then the frozen spherical particles were dissolved by low-temperature saturated $KHCO_3$ aqueous solution. The ice scaffolding was dissolved and microparticles of $KHCO_3$ with size below 100 μm were collected.

Comparing with the freeze-dissolving in antisolvent method, the new freeze-dissolving in saturated solution method only requires one solvent, which can be rapidly applied in many more systems without searching for compatible new antisolvent. Comparing with the freeze-drying method, both the freeze-dissolving methods can produce $KHCO_3$ microparticles of similar size distribution without using specific facility of vacuum, and with 99% reduction in both time consumption and energy usage.

Author contributions

Jiaqi Luo: data curation, visualization, investigation, validation, writing – original draft. Qifan Su: writing – review & editing. Xinyue Zhai: formal analysis, investigation, methodology. Yuan Zou: writing – review & editing. Qiushuo Yu: conceptualization, methodology, writing – review & editing, funding acquisition. Huaiyu Yang: conceptualization, methodology, writing – review & editing, funding acquisition.

Conflicts of interest

The authors declare that they have no known competing financial interests or personal relationships that could have appeared to influence the work reported in this paper.

Acknowledgements

The authors are grateful to the National Science Foundation (NSFC21978234) for financial assistance in this project.

Notes and references

1 L.-M. Xu, T.-T. Hu, Y. Pu, Y. Le, J.-F. Chen and J.-X. Wang, *Chem. Eng. J.*, 2014, **252**, 281–287.
2 Y. Bayat and V. Zeynali, *J. Energ. Mater.*, 2011, **29**, 281–291.
3 R. Kumar, P. F. Siril and P. Soni, *Propellants, Explos., Pyrotech.*, 2014, **39**, 383–389.
4 F. Nie, J. Zhang, Q. Guo, Z. Qiao and G. Zeng, *J. Phys. Chem. Solids*, 2010, **71**, 109–113.
5 V. Stepanov, V. Anglade, W. A. B. Hummers, A. V. Bezmelnitsyn and L. N. Krasnoperov, *Propellants, Explos., Pyrotech.*, 2011, **36**, 240–246.
6 N. Mezzomo, S. R. Rosso Comim, C. E. M. Campos and S. R. S. Ferreira, *Powder Technol.*, 2015, **270**, 378–386.
7 K. Donaldson, D. Brown, A. Clouter, R. Duffin, W. MacNee, L. Renwick, L. Tran and V. Stone, *J. Aerosol Med.*, 2002, **15**, 213–220.
8 C. Monteiller, L. Tran, W. MacNee, S. Faux, A. Jones, B. Miller and K. Donaldson, *Occup. Environ. Med.*, 2007, **64**, 609–615.
9 Q. S. Yu, W. Y. Jia, J. J. Pu, Y. C. Wang and H. Y. Yang, *Chem. Eng. Sci.*, 2021, **229**, 116082.
10 C. M. Keck and R. H. Muller, *Eur. J. Pharm. Biopharm.*, 2006, **62**, 3–16.
11 V. B. Patravale, A. A. Date and R. M. Kulkarni, *J. Pharm. Pharmacol.*, 2010, **56**, 827–840.

12 M. Kakran, R. Shegokar, N. G. Sahoo, L. Al Shaal, L. Li and R. H. Müller, *Eur. J. Pharm. Biopharm.*, 2012, **80**, 113–121.
13 A. H. L. Chow, H. H. Y. Tong, P. Chattopadhyay and B. Y. Shekunov, *Pharm. Res.*, 2007, **24**, 411–437.
14 H. Mansour, X. Wu, D. Hayes, J. B. Zwischenberger and R. Kuhn, *Drug Des., Dev. Ther.*, 2013, **7**, 59–72.
15 Y. H. Kim and K. S. Shing, *Powder Technol.*, 2008, **182**, 25–32.
16 A. Jaworek, *Powder Technol.*, 2007, **176**, 18–35.
17 I. Zbicinski, I. Smucerowicz, C. Strumillo and C. Crowe, *Braz. J. Chem. Eng.*, 2000, **17**, 441–450.
18 J. Thies and B. W. Müller, *Eur. J. Pharm. Biopharm.*, 1998, **45**, 67–74.
19 R. Ghaderi, P. Artursson and J. Carlfors, *Eur. J. Pharm. Sci.*, 2000, **10**, 1–9.
20 T. K. Maiti, P. Dixit, A. Suhag, S. Bhushan, A. Yadav, N. Talapatra and S. Chattopadhyay, *RSC Sustain.*, 2023, **1**, 665–697.
21 M. Négrier, E. El Ahmar, R. Sescousse, M. Sauceau and T. Budtova, *RSC Sustain.*, 2023, **1**, 335–345.
22 Q. S. Yu, Y. C. Wang, J. Q. Luo and H. Y. Yang, *ACS Sustain. Chem. Eng.*, 2022, **10**, 7825–7832.
23 J. Q. Luo, Q. F. Su, Q. S. Yu, X. Y. Zhai, Y. Zou and H. Y. Yang, *Green Chem. Eng.*, 2023, DOI: **10.1016/j.gce.2023.07.003**.
24 X. H. Zhang, Z. X. Wei, H. Choi, H. Hao and H. Y. Yang, *Adv. Mater. Interfaces*, 2021, **8**, 2001200.
25 H. Y. Yang and Å. C. Rasmuson, *Fluid Phase Equilib.*, 2014, **376**, 69–75.
26 L. P. Wang, Y. Bao, Z. Sun, V. J. Pinfield, Q. X. Yin and H. Y. Yang, *Ind. Eng. Chem. Res.*, 2021, **60**, 4110–4119.
27 H. Y. Yang, B. D. Belviso, X. Y. Li, W. Q. Chen, T. F. Mastropietro, G. Di Profio, R. Caliandro and J. Y. Y. Heng, *Crystals*, 2019, **9**, 230.
28 K. Q. Kuang, W. K. Chow, X. M. Ni, D. L. Yang, W. R. Zeng and G. X. Liao, *Fire Mater.*, 2011, **35**, 353–366.
29 J. H. Zhou, H. P. Jiang, Y. H. Zhou and W. Gao, *Process Saf. Environ. Prot.*, 2019, **132**, 303–312.
30 J. Z. Jia, X. Y. Tian and F. X. Wang, *ACS Omega*, 2022, **7**, 31974–31982.